Finite energy chiral sum rules and τ spectral functions

M. Davier* and A. Höcker†
Laboratoire de l'Accélérateur Linéaire, IN2P3-CNRS et Université de Paris-Sud, F-91405 Orsay, France

L. Girlanda‡ and J. Stern§
Division de Physique Théorique, Institut de Physique Nucléaire, Université de Paris-Sud, F-91406 Orsay, France
(Received 4 May 1998; published 7 October 1998)

A combination of finite energy sum rule techniques and chiral perturbation theory (χPT) is used in order to exploit recent ALEPH data on the non-strange τ vector (V) and axial-vector (A) spectral functions with respect to an experimental determination of the χPT quantity L_{10}. A constrained fit of $R^{(k,l)}_{\tau,V-A}$ inverse moments ($l<0$) and positive spectral moments ($l\geqslant 0$) adjusts simultaneously L_{10} and the nonperturbative power terms of the operator product expansion. We give explicit formulas for the first $k=0,1$ and $l=-1$ non-strange inverse moment chiral sum rules to one-loop order generalized χPT. Our final result reads $L^r_{10}(M_\rho)=-(5.13\pm 0.19)\times 10^{-3}$, where the error includes experimental and theoretical uncertainties. [S0556-2821(98)07221-X]

PACS number(s): 11.55.Hx, 12.38.Lg, 12.39.Fe, 13.35.Dx

I. INTRODUCTION

The nonperturbative features of strong interactions make QCD a rich environment for theoretical investigations. At sufficiently high energies it is possible to parametrize the nonperturbative effects by vacuum condensates, following the rules of Wilson's operator product expansion (OPE) [1]. The universal character of these condensates has been used in the derivation of the so-called QCD spectral sum rules [2] allowing, in principle, their determination from experiment. A particular role is played by the condensates which are order parameters of the spontaneous breakdown of chiral symmetry (SBχS). The latter vanish at all orders of perturbation theory and they control the high energy behavior of chiral correlation functions, such as the difference of vector and axial vector current two-point functions. On the other hand, at low energies, SBχS makes it possible to construct an effective theory of QCD, the chiral perturbation theory (χPT) [3,4], which uses the Goldstone bosons as fundamental fields and provides a systematic expansion of QCD correlation functions in powers of momenta and quark masses. All missing information is then parametrized by low-energy coupling constants, which can be determined phenomenologically in low-energy experiments involving pions and kaons. The fundamental parameters describing chiral symmetry breaking, the running quark masses and the quark anti-quark condensates $\langle\bar{q}q\rangle$ appear both in low-energy (χPT) and the high energy OPE expansion. For this reason it is useful to combine the two expansions in order to get a truly systematic approach to the chiral sum rules [5]. In this paper the combined approach is illustrated through a determination of the L_{10} constant of the chiral Lagrangian, including high-energy corrections coming from the OPE. The connection between the two domains is provided by experimental data on τ hadronic spectral functions published recently by the ALEPH Collaboration [6,7].

At the leading order of χPT, L_{10} is directly linked to the vector, v_1, and axial-vector, a_1, spin-one spectral functions (the subscripts refer to the spin J of the hadronic system) through the Das-Mathur-Okubo (DMO) sum rule [8]

$$\frac{1}{4\pi^2}\int_0^{s_0\to\infty} ds\,\frac{1}{s}[v_1(s)-a_1(s)]\simeq -4L_{10}. \qquad (1)$$

As it stands the DMO sum rule (1) is subject to chiral corrections due to non-vanishing quark masses [9]. On the other hand, the integral has to be cut at some finite energy $s_0\leqslant M_\tau^2$, since no experimental information on v_1-a_1 is available above M_τ^2. This truncation introduces an error which competes with the low-energy chiral corrections. Both types of corrections can be systematically included through (i) the high-energy expansion in $\alpha_s(s_0)$ and in inverse powers of s_0, and (ii) the low-energy expansion in powers of quark masses and of their logarithms.

II. SPECTRAL MOMENTS

Using unitarity and analyticity, the spectral functions are connected to the imaginary part of the two-point correlation functions,

$$\Pi^{\mu\nu}_{ij,U}(q)\equiv i\int d^4x e^{iqx}\langle 0|T(U^\mu_{ij}(x)U^\nu_{ij}(0)^\dagger)|0\rangle$$
$$=(-g^{\mu\nu}q^2+q^\mu q^\nu)\Pi^{(1)}_{ij,U}(q^2)+q^\mu q^\nu\Pi^{(0)}_{ij,U}(q^2), \qquad (2)$$

of vector ($U^\mu_{ij}\equiv V^\mu_{ij}=\bar{q}_j\gamma^\mu q_i$) or axial-vector ($U^\mu_{ij}\equiv A^\mu_{ij}=\bar{q}_j\gamma^\mu\gamma_5 q_i$) color-singlet quark currents for time-like momentum-squared $q^2>0$. Lorentz decomposition is used to separate the correlation function into its $J=1$ and $J=0$ parts. The correlation function (2) is analytic everywhere in the complex s plane except on the positive real axis where sin-

*Email address: davier@lal.in2p3.fr
†Email address: hoecker@lal.in2p3.fr
‡Email address: girlanda@ipno.in2p3.fr
§Email address: stern@ipno.in2p3.fr

gularities exist. Using the definitions adopted in Refs. [6,7] together with Eq. (2), one identifies, for non-strange quark currents,

$$\text{Im}\,\Pi^{(1)}_{ud,V/A}(s)=\frac{1}{2\pi}v_1/a_1(s),\quad \text{Im}\,\Pi^{(0)}_{ud,A}(s)=\frac{1}{2\pi}a_0(s). \tag{3}$$

Due to the conserved vector current, there is no $J=0$ contribution to the vector spectral function, while the only contribution to a_0 is assumed to be from the pion pole. It is connected via PCAC to the pion decay constant, $a_{0,\pi}(s)=4\pi^2 f_\pi^2\delta(s-m_\pi^2)$.

According to the method proposed by Le Diberder and Pich [10], it is possible to exploit the information from the explicit shape of the spectral functions by calculating so-called spectral moments, i.e., weighted integrals over the spectral functions. If $W(s)$ is an analytic function, by Cauchy's theorem, the imaginary part of $\Pi^{(J)}_{ij,\text{V/A}}$ is proportional to the discontinuity across the positive real axis:

$$\int_0^{s_0} ds W(s)\,\text{Im}\,\Pi^{(J)}_{ij,\text{V/A}}(s)=-\frac{1}{2i}\oint_{|s|=s_0} ds W(s)\Pi^{(J)}_{ij,\text{V/A}}(s), \tag{4}$$

where s_0 is large enough for the OPE series to converge. The authors of Ref. [10] choose for $W(s)$ the functions

$$W^{(k,l)}(s)=\left(1-\frac{s}{s_0}\right)^{2+k}\left(\frac{s}{s_0}\right)^l, \tag{5}$$

with k and l positive integers. The factor $(1-s/s_0)^k$ suppresses the integrand at the crossing of the positive real axis where the validity of the OPE is questioned. Its counterpart $(s/s_0)^l$ projects on higher energies. These moments were successfully applied in order to constrain nonperturbative contributions to the τ hadronic width, R_τ, a procedure which led to precise determinations of $\alpha_s(M_\tau^2)$ [7,11,12].

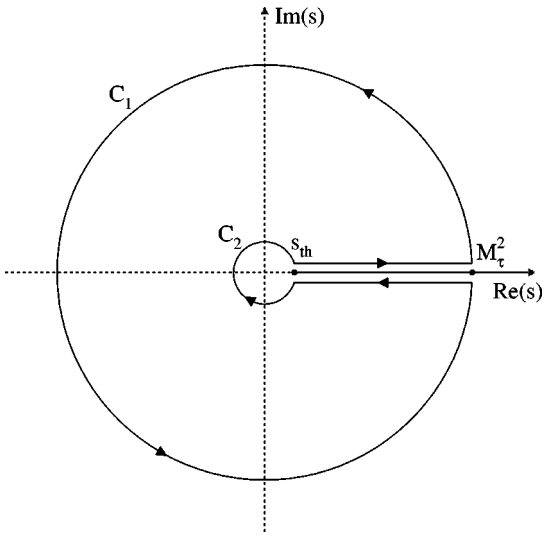

FIG. 1. Integration contour around the circles at $s=M_\tau^2$ and $s=s_{\text{th}}$.

The extension of the spectral moment analysis to negative integer values of l [''inverse moment sum rules'' (IMSR) [13]] requires, due to the pole at $s=0$, a modified contour of integration in the complex s plane, as shown in Fig. 1. This is where χPT comes into play: along the small circle placed at the production threshold, $s_{\text{th}}=4M_\pi^2$, we can use χPT predictions for the two-point correlators.

Using the weight function (5) we adopt the following definition of the moments:

$$R^{(k,l)}_{\tau,V/A}\equiv 12\pi|V_{ud}|^2 S_{\text{EW}}\int_{s_{\min}}^{M_\tau^2}\frac{ds}{M_\tau^2}\left(1-\frac{s}{M_\tau^2}\right)^{2+k}\left(\frac{s}{M_\tau^2}\right)^l\left[\left(1+2\frac{s}{M_\tau^2}\right)\text{Im}\,\Pi^{(0+1)}_{V/A}(s)-\frac{2s}{M_\tau^2}\,\text{Im}\,\Pi^{(0)}_{A}(s)\right], \tag{6}$$

where $s_{\min}=0$ for the positive moments[1] ($l\geqslant 0$) and $s_{\min}=s_{\text{th}}$, which is the continuum threshold, for the inverse moments. According to the relation (4), Eq. (6) reads

$$R^{(k,l)}_{\tau,V/A}=6\pi i|V_{ud}|^2 S_{\text{EW}}\oint_C\frac{ds}{M_\tau^2}\left(1-\frac{s}{M_\tau^2}\right)^{2+k}\left(\frac{s}{M_\tau^2}\right)^l\left[\left(1+2\frac{s}{M_\tau^2}\right)\Pi^{(0+1)}_{V/A}(s)-2\frac{s}{M_\tau^2}\Pi^{(0)}_{A}(s)\right], \tag{7}$$

where $C=C_1+C_2$ for the inverse moments and $C=C_1$ for the positive moments (see Fig. 1).

Due to the cut of the integral (6) at M_τ^2, nonperturbative physics parametrized by the short-distance OPE for scalar operators [1,2,14] must be considered:

$$\Pi^{(J)}_{V/A}(s)=\sum_{D=0,2,4,\ldots}\frac{1}{(-s)^{D/2}}\sum_{\dim\mathcal{O}=D}C^{(J)}_{V/A}(s,\mu^2)\langle\mathcal{O}_{V/A}(\mu^2)\rangle. \tag{8}$$

The parameter μ separates the long-distance nonperturbative effects, absorbed into the vacuum expectation elements $\langle\mathcal{O}_{V/A}(\mu^2)\rangle$, from the short-distance effects which are included in the Wilson coefficients $C_{V/A}(s,\mu^2)$ [1]. We will assume the

[1]This is due to the pion pole which is at zero mass in the chiral limit.

convergence of the OPE series at the τ mass. This is justified in the light of the success of the analysis performed in Ref. [7] (see Ref. [15] for details). Using the formulas of Refs. [14] and [16] for the nonperturbative power expansion of the correlators, one obtains for the $(V-A)$ case

$$\Pi^{(0+1)}_{ud,V-A}(-s) = -\frac{a_s(s)}{\pi^2}\frac{\hat{m}^2(s)}{s} - \frac{16}{7\pi^2}\frac{\hat{m}^4(s)}{s^2} + \left(\frac{8}{3}a_s(s) + \frac{59}{3}a_s^2(s)\right)\frac{\hat{m}\langle\bar{u}u+\bar{d}d\rangle}{s^2}$$
$$-8\pi^2 a_s(\mu^2)\left[1+\left(\frac{119}{24}-\frac{1}{2}L(s)\right)a_s(\mu^2)\right]\frac{\langle\mathcal{O}_6^1(\mu^2)\rangle}{s^3} + \frac{2\pi^2}{3}[3+4L(s)]a_s^2(\mu^2)\frac{\langle\mathcal{O}_6^2(\mu^2)\rangle}{s^3} + \frac{\langle\mathcal{O}_8\rangle}{s^4}, \quad (9)$$

$$\Pi^{(0)}_{ud,V-A}(-s) = -\frac{3}{\pi^2}\left[2a_s^{-1}(s) - 5 + \left(\frac{75}{17}\zeta(3) - \frac{21373}{2448}\right)a_s(s)\right]\frac{\hat{m}^2(s)}{s} - 4\hat{C}(\mu^2)\frac{\hat{m}^2(\mu^2)}{s}$$
$$-\frac{1}{7\pi^2}\left[\frac{53}{2} - 12a_s^{-1}(s)\right]\frac{\hat{m}^4(s)}{s^2} - 2\frac{\hat{m}\langle\bar{u}u+\bar{d}d\rangle}{s^2}, \quad (10)$$

with $a_s(s)=\alpha_s(s)/\pi$, $L(s)=\log(s/\mu^2)$ and the dimension $D=6$ operators

$$\mathcal{O}_6^1 \equiv \bar{u}\gamma_\mu\gamma_5 T^a d\,\bar{d}\gamma^\mu\gamma_5 T^a u - \bar{u}\gamma_\mu T^a d\,\bar{d}\gamma^\mu T^a u$$
$$\mathcal{O}_6^2 \equiv \bar{u}\gamma_\mu \bar{d}d\,\gamma^\mu u - \bar{u}\gamma_\mu\gamma_5 d\,\bar{d}\gamma^\mu\gamma_5 u, \quad (11)$$

where the $SU(3)$ generators T^a are normalized so that $\mathrm{tr}(T^aT^b)=\delta^{ab}/2$. We use the average mass $\hat{m}\equiv(m_u+m_d)/2$ in the above equations, i.e., we assume $SU(2)$ symmetry. The constant $\hat{C}(\mu^2)$ depends on the renormalization procedure[2] and should not affect physical observables. The dimension $D=0$ contribution is of pure perturbative origin and is degenerate in all orders of perturbation theory for vector and axial-vector currents. Dimension $D=2$ mass terms are calculated perturbatively to order α_s^2 which suffices for the light u,d, quarks. Possible $1/s$ contributions coming from ultraviolet renormalons (see, e.g., Refs. [17,18]), are expected to vanish in the $V-A$ difference, similar to what happens for the $D=0$ contribution, since they are of perturbative origin. The coefficient functions of the dimension $D=4$ operators for vector and axial-vector currents have been calculated to subleading order in Refs. [19,20]. Their vacuum expectation values are expressed in terms of the scale invariant gluon and quark condensates. Since the Wilson coefficients of the gluon condensate are symmetric for vector and axial-vector currents, they vanish in the difference. The expectation values of the dimension $D=6$ operators (11) obey the inequalities $\langle\mathcal{O}_6^1(\mu^2)\rangle\geqslant 0$ and $\langle\mathcal{O}_6^2(\mu^2)\rangle\leqslant 0$, which can be derived from first principles. The corresponding coefficient functions were calculated by the authors of Ref. [21] in the chiral limit for which the $J=0$ contribution vanishes. For the dimension $D=8$ operators no such calculations are available in the literature, and we will assume that there is no logarithmic s dependence in leading order α_s. Again, the $J=0$ contribution vanishes in the chiral limit.

As constraints on the nonperturbative phenomenological operators introduced in Eqs. (9) and (10) from theory alone are scarce, we will benefit from the information provided by the $(V-A)$ spectral moments in order to determine the magnitude of the OPE power terms at M_τ^2. We therefore perform a combined fit of the IMSR (i.e., $l=-1$) which determines L_{10}, and the $l\geqslant 0$ moments which adjust the nonperturbative contributions.

[2]We will assume a renormalization scheme that preserves chiral symmetry, so that $\hat{C}$ is the same for the vector and axial correlators.

III. CHIRAL PERTURBATION THEORY

The non-strange correlators (2) have been calculated at one-loop level [4,22] and, most recently, at two-loop level [23,24] in standard χPT. In this paper we stick to the $O(p^4)$ one-loop order for the following two reasons: (i) the high energy corrections are often more important than the $O(p^6)$ chiral corrections (whose precise estimate has not yet been fully completed [9]) and (ii) it is important to proceed in the combined analysis order by order in quark masses. On the other hand, we use the generalized version of χPT (GχPT) [25], which allows us to investigate the sensitivity of the analysis to the variation of the quark condensate and of the quark mass ratio $r=m_s/\hat{m}$. The standard χPT assumes [26] $2\hat{m}\langle\bar{q}q\rangle\simeq -F_\pi^2M_\pi^2$ and $r\simeq 2M_K^2/M_\pi^2-1\simeq 25.9$, whereas G$\chi$PT admits lower values of these two quantities [27,25]. It is interesting to investigate whether the ALEPH spectral function data are precise enough to have any impact on the ongoing debate about the size of $\langle\bar{q}q\rangle$. Anyhow, the alterations of the standard $O(p^4)$ results for non-strange correlators (2) introduced by GχPT are marginal. They merely concern the symmetry breaking $J=0$ component of the spectral functions and most of them are actually absorbed into the renormalization of F_π.

In order to make our analysis as independent of a particular truncation of the χPT series as possible, we proceed in two steps. First, one defines a phenomenological quantity

called $L_{10}^{\rm eff}$ via the contribution of the small circle C_2 (see Fig. 1) to the integral (7) of the chiral combination $V-A$ for $l=-1$. $L_{10}^{\rm eff}$ is then determined in the combined fit of the IMSR and $l\geqslant 0$ moments. The result of this fit is independent of the χPT renormalization scale $\mu_{\chi\rm PT}$. The latter is used in the next step in order to relate $L_{10}^{\rm eff}$ to the quark-mass independent, scale dependent constant $L_{10}^r(\mu_{\chi\rm PT})$ and finally to other observables (from $\pi\to e\nu\gamma$ data, $\langle r^2\rangle_\pi$).

The isospin two-point correlators at one loop in GχPT read

$$\Pi_{ud,V}^{(0+1)}(s)=4M_{KK}^r(s)+8M_{\pi\pi}^r(s)-4(L_{10}^r+2H_1^r), \tag{12}$$

$$\Pi_{ud,V}^{(0)}(s)=0, \tag{13}$$

$$\Pi_{ud,A}^{(0+1)}(s)=-\frac{2F_\pi^2}{s-M_\pi^2}-4(2H_1^r-L_{10}^r), \tag{14}$$

$$s\Pi_{ud,A}^{(0)}(s)=-\frac{2F_\pi^2M_\pi^2}{s-M_\pi^2}+8\hat{m}^2(H_{2,2}-2B_3). \tag{15}$$

The functions $M_{PP'}^r(s)$ are loop integrals, defined, e.g., in Ref. [22]. The superscript r refers to renormalized quantities, which depend on the scale $\mu_{\chi\rm PT}$. The whole expressions are $\mu_{\chi\rm PT}$ independent. $H_{2,2}$ and B_3 are found to be finite, in agreement with [28], and do not need renormalization. H_1^r and $H_{2,2}$ are coefficients of contact terms of the sources. They are counterterms needed to renormalize the ultraviolet divergences of the Green functions and do not appear in physical observables. Our aim is to determine L_{10}: therefore we will consider the difference between the vector and the axial-vector correlators for which the constant H_1 disappears. Correspondingly, as already pointed out, we will not need the perturbative expressions which are identical for vector and axial-vector cases. As for the constant $H_{2,2}$ which multiplies the term

$$\langle D_\mu\chi^\dagger D^\mu\chi\rangle$$

of the $\mathcal{L}_{(2,2)}$ chiral Lagrangian,[3] it always appears in the same combination with $\hat{C}(\mu^2)$, in such a way that the ambiguities cancel out. We thus define a $\hat{H}_{2,2}$, in which the constant $\hat{C}(M_\tau^2)$ is absorbed. What is new at this order with respect to SχPT is the appearance of the constant B_3 which multiplies the term

$$\langle U^\dagger D_\mu\chi U^\dagger D_\mu\chi+\text{H.c.}\rangle$$

of the $\mathcal{L}_{(2,2)}$ Lagrangian. As can be seen from its form it is difficult to find a process in which B_3 would contribute directly. It will contribute to off-shell vertices involving Goldstone bosons.

The IMSR's corresponding to $l=-1$ and $k=0,1$ read

$$\begin{aligned}\frac{1}{|V_{ud}|^2S_{\rm EW}}R_{\tau,V-A}^{(0,-1)}=&-96\pi^2L_{10}^{\rm eff}+24\pi^2\frac{F_\pi^2M_\pi^2}{M_\tau^4}+\frac{144}{M_\tau^2}\hat{m}^2(M_\tau^2)\left[\frac{1}{a_s(M_\tau^2)}-\frac{23}{8}+\left(\frac{\pi^2}{12}-\frac{36061}{4896}+\frac{75}{34}\zeta(3)\right)a_s(M_\tau^2)\right]\\&+\frac{96}{M_\tau^4}\pi^2\hat{m}\langle\bar{d}d+\bar{u}u\rangle\left[1+a_s(M_\tau^2)+\frac{17}{2}a_s^2(M_\tau^2)\right]-\frac{576}{7M_\tau^4}\hat{m}^4(M_\tau^2)\left[\frac{1}{a_s(M_\tau^2)}-\frac{29}{24}\right]-\frac{192\pi^4}{M_\tau^6}a_s(\mu^2)\\&\times\left[1+\left(\frac{103}{24}-\frac{L(M_\tau^2)}{2}\right)a_s(\mu^2)\right]\langle\mathcal{O}_6^1(\mu^2)\rangle+\frac{400\pi^4}{3M_\tau^6}a_s^2(\mu^2)\left(1+\frac{12}{25}L(M_\tau^2)\right)\langle\mathcal{O}_6^2(\mu^2)\rangle,\end{aligned} \tag{16}$$

$$\begin{aligned}\frac{1}{|V_{ud}|^2S_{\rm EW}}R_{\tau,V-A}^{(1,-1)}=&-96\pi^2L_{10}^{\rm eff}-24\pi^2\left(\frac{F_\pi^2}{M_\tau^2}-3\frac{F_\pi^2M_\pi^2}{M_\tau^4}+\frac{F_\pi^2M_\pi^4}{M_\tau^6}\right)+\frac{144}{M_\tau^2}\hat{m}^2(M_\tau^2)\left[\frac{1}{a_s(M_\tau^2)}-\frac{71}{24}\right.\\&\left.+\left(\frac{\pi^2}{12}-\frac{39461}{4896}+\frac{75}{34}\zeta(3)\right)a_s(M_\tau^2)\right]+\frac{144}{M_\tau^4}\pi^2\hat{m}\langle\bar{d}d+\bar{u}u\rangle\left[1+\frac{2}{3}a_s(M_\tau^2)+\frac{43}{6}a_s^2(M_\tau^2)\right]\\&-\frac{864}{7M_\tau^4}\hat{m}^4(M_\tau^2)\left[\frac{1}{a_s(M_\tau^2)}-\frac{2}{3}\right]-\frac{480\pi^4}{M_\tau^6}a_s(\mu^2)\left[1+\left(\frac{581}{120}-\frac{L(M_\tau^2)}{2}\right)a_s(\mu^2)\right]\langle\mathcal{O}_6^1(\mu^2)\rangle\\&+\frac{472\pi^4}{3M_\tau^6}a_s^2(\mu^2)\left(1+\frac{60}{59}L(M_\tau^2)\right)\langle\mathcal{O}_6^2(\mu^2)\rangle+24\pi^2\frac{\langle\mathcal{O}_8\rangle}{M_\tau^8}.\end{aligned} \tag{17}$$

[3] $\mathcal{L}_{(n,m)}$ collects terms in the chiral Lagrangian with n covariant derivatives and m powers of quark masses. In the same notation the H_1 constant introduced by Gasser and Leutwyler [22] would become $H_{4,0}$.

Notice that in the $D=2$ contribution we have not taken into account the α_s^2 term, which is known for the transversal correlator (9), but not for the scalar correlator (10). The contribution of the latter to the contour integral is non-zero for the inverse moments, unlike for the positive ones. We have defined

$$-8L_{10}^{\rm eff}=\lim_{s\to 0}\left\{\left(1+\frac{2s}{M_\tau^2}\right)\Pi_{ud,{\rm V-A}}^{(0+1)}(s)-\frac{2s}{M_\tau^2}\Pi_{ud,{\rm V-A}}^{(0)}(s)-\frac{2F_\pi^2}{s-M_\pi^2}-4\frac{F_\pi^2}{M_\tau^2}\right\}+8\frac{\hat{m}^2(M_\tau^2)}{M_\tau^2}\hat{C}(M_\tau^2), \qquad (18)$$

which is proportional to the contribution of the small circle C_2 to the integral (7), with the pion pole subtracted. This quantity is a well defined observable, the ambiguity in the two-point function being absorbed by the constant $\hat{C}$. In the particular case of the one-loop GχPT calculation, its expansion reads

$$L_{10}^{\rm eff}=L_{10}^r(\mu_{\chi{\rm PT}})+\frac{1}{128\pi^2}\left(\log\frac{M_\pi^2}{\mu_{\chi{\rm PT}}^2}+1\right)+\frac{1}{384\pi^2}\log\frac{M_K^2}{M_\pi^2}+\frac{2\hat{m}^2}{M_\tau^2}(2B_3-\hat{H}_{2,2}), \qquad (19)$$

which is independent of $\mu_{\chi{\rm PT}}$. Unless stated otherwise all condensates, quark masses and χPT constants in the above expressions are evaluated at QCD renormalization scale $\mu_{\rm QCD}=M_\tau$, while the product of the light quark mass and the scalar quark operator, $\hat{m}\langle\bar{d}d+\bar{u}u\rangle$, is scale invariant. Taking the difference of Eqs. (16) and (17) and subtracting the contribution from the pion pole recovers the expression for $R_{\tau,V-A}=R_{\tau,V-A}^{(0,0)}$ given in [14]. Due to the strong intrinsic correlations of 98% between the IMSR's defined above only one IMSR is used as input to the combined fit. We find it convenient to use the moment $k=1$, $l=-1$ [Eq. (17)] because its experimental value is known with a 30% better precision which is due to the additional $(1-s/M_\tau^2)$ suppression of the less accurate high energy tail of the $(V-A)$ spectral function.

IV. THEORETICAL PARAMETERS AND UNCERTAINTIES

When fitting the theoretical prediction of the $R_{\tau,V-A}^{(k,l)}$ moments to data, theoretical as well as experimental uncertainties and the correlations of these between the (k,l) moments must be considered. The masses of the light quarks are parametrized using the mass ratio $r=m_s/\hat{m}$ of which the central value is set to the SχPT value of 26. A lower limit is found at $r\geqslant r_{\rm limit}=2(M_K/M_\pi)-1\approx 6.1$ (while $r_{\rm limit}\approx 8.2$ when including higher orders [29]) which determines the range

$$8<r<\infty.$$

The average light quark mass is then obtained via $\hat{m}=m_s/r$ where we use for the strange quark mass $m_s(M_\tau)=172\ {\rm MeV}/c^2$ [30]. This parametrization makes it possible to use the theoretical correlation between $\hat{m}$ and the quark condensate, which to leading order in quark masses is given by the generalized Gell-Mann–Oakes–Renner relation [27,25]:

$$\hat{m}\langle\bar{u}u+\bar{d}d\rangle\simeq -F_\pi^2M_\pi^2\frac{(r-r_1)(r+r_1+2)}{r^2-1}, \qquad (20)$$

where $r_1\simeq 2(M_K/M_\pi)-1$. For the standard value $r=25.9$, Eq. (20) becomes the usual PCAC (partial conservation of axial vector current) relation $\hat{m}\langle\bar{u}u+\bar{d}d\rangle=-F_\pi^2M_\pi^2$. Corrections to Eq. (20) are expected to be small in the whole range of r so that we assume a relative uncertainty of 10%. We will comment in Sec. VI on the sensitivity of the data with respect to the r ratio. Theoretical uncertainties are introduced from the strong coupling constant where, in order to be uncorrelated to the τ data used in this analysis, we rely on the result from the global electroweak fit found recently to be [31,32]

$$\alpha_s(M_Z^2)=0.1198\pm 0.0031.$$

Uncertainties from the OPE separation scale μ are evaluated by varying μ from 1.3 GeV to 2.3 GeV, while in the fit we choose $\mu=M_\tau$ so that the logarithmic scale dependence of the dimension $D=6$ terms vanishes after the contour integration. Additional small uncertainties stem from the pion decay constant, $F_\pi=(92.4\pm 0.2)$ MeV, taken from Ref. [33] and the overall correction factor for electroweak radiation, $S_{\rm EW}=1.0194$, obtained in Ref. [34], with an estimated error of $\Delta S_{\rm EW}=0.0040$ according to Ref. [35].

An overview of the associated uncertainties in the theoretical prediction of the moments is given in Table I. The moment errors from the α_s uncertainty depend on the central input values of the nonperturbative operators. The numbers given in the fourth line of Table I correspond to the fit values, Eqs. (25), (26), which have been obtained in an iterative procedure.

V. SPECTRAL FUNCTIONS FROM HADRONIC τ DECAYS

The ALEPH Collaboration measured the inclusive invariant mass-squared spectra of vector and axial-vector hadronic τ decays and provided the corresponding bin-to-bin covariance matrices [6,7]. The mass distributions naturally contain the kinematic factor of Eq. (6) so that the measured spectral moments read

$$R_{\tau,V-A}^{(k,l)}=\int_0^{M_\tau^2}ds\left(1-\frac{s}{M_\tau^2}\right)^k\left(\frac{s}{M_\tau^2}\right)^l\left[B_V\frac{dN_V}{N_V ds}-B_A\frac{dN_A}{N_A ds}\right]\frac{1}{B_e}, \qquad (21)$$

TABLE I. Measured spectral moments of vector (V) minus axial-vector (A) using τ data only (ALEPH) and using $\tau+e^+e^-$ data (ALEPH+NA7). The quoted errors account for the total experimental uncertainties including statistical and systematic effects as well as the theoretical uncertainties according to Sec. IV. The last line gives the fitted theoretical moments using the parameters given in Eqs. (24)–(26).

$(k,l)\rightarrow$	$(1,-1)$	$(0,0)$	$(1,0)$	$(1,1)$	$(1,2)$	$(1,3)$
$R^{(k,l)}_{\tau,V-A}$ (ALEPH)	5.16	0.055	0.038	0.047	−0.0164	−0.0126
$\Delta^{\rm exp}R^{(k,l)}_{\tau,V-A}$	0.09	0.031	0.017	0.006	0.0035	0.0023
$R^{(k,l)}_{\tau,V-A}$ (ALEPH+NA7)	5.13	0.055	0.037	0.047	−0.0164	−0.0126
$\Delta^{\rm exp}R^{(k,l)}_{\tau,V-A}$	0.08	0.031	0.017	0.006	0.0035	0.0023
$\Delta^{\rm theo}R^{(k,l)}_{\tau,V-A}$ (Δr)	0.12	0.003	0.003	0.001	0.0003	<0.0001
$\Delta^{\rm theo}R^{(k,l)}_{\tau,V-A}$ $(\Delta\alpha_s)$	0.02	0.009	0.009	0.002	0.0029	0.0001
$\Delta^{\rm theo}R^{(k,l)}_{\tau,V-A}$ $(\Delta S_{\rm EW})$	0.02	<0.001	<0.001	<0.001	0.0001	<0.0001
$\Delta^{\rm theo}R^{(k,l)}_{\tau,V-A}$ $(\Delta\mu_{\rm OPE})$	<0.01	0.005	0.005	0.002	0.0018	<0.0001
$\Delta^{\rm theo}R^{(k,l)}_{\tau,V-A}$ $(\Delta\langle\bar{q}q\rangle)$	<0.01	<0.001	<0.001	<0.001	<0.0001	<0.0001
$\Delta^{\rm theo}R^{(k,l)}_{\tau,V-A}$ (ΔF_π)	<0.01	<0.001	<0.001	<0.001	<0.0001	<0.0001
$R^{(k,l)}_{\tau,V-A}$ (Theory fitted)	5.13	0.061	0.032	0.053	−0.0148	−0.0098

with the normalized invariant mass-squared spectra $(1/N_{V/A})(dN_{V/A}/ds)$ of vector and axial-vector final states, the electronic branching ratio (using universality) [33,7], $B_e=(17.794\pm0.045)\%$, and the inclusive branching ratios [7], $B_V=(31.58\pm0.29)\%$, $B_A=(30.56\pm0.30)\%$, as well as their difference, $B_{V-A}=(1.02\pm0.58)\%$. Due to anticorrelations between vector and axial-vector final states, especially for the $K\bar{K}\pi$ modes where the vector and axial-vector parts are unknown, the error of the difference is larger than the quadratic sum of the errors on V and A. Figure 2 shows the $(V-A)$ mass-squared distribution, which is the integrand of Eq. (21) for zero moments, $k=l=0$. With increasing masses it is dominated by the ρ (V), a_1 (A) and the $\rho(1450)$, $\omega\pi$ (V) resonance contributions which create the oscillating behavior. Tables I and II give the experimental values and uncertainties for the IMSR $R_{\tau,V-A}$ and the $k=1$, $l=0,\ldots,3$

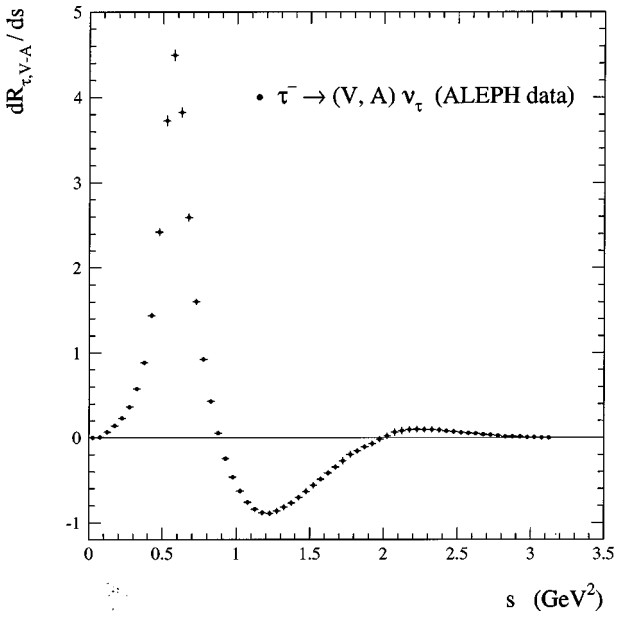

FIG. 2. Vector minus axial-vector $(V-A)$ invariant mass-squared distribution measured by ALEPH [7].

moments as well as their correlations which are computed analytically from the contraction of the derivatives of the moments with the covariance matrices of the respective normalized invariant mass-squared spectra.

Based on isospin invariance, the conserved vector current (CVC) hypothesis relates vector hadronic τ spectral functions to isovector cross section measurements of the reaction $e^+e^-\rightarrow$hadrons. There exist precise data on the low energy, time-like pion form factor-squared $|F_\pi(s)|^2$ measured by the NA7 Collaboration [36]. Using the CVC relation

$$v_{1,\pi^-\pi^0}(s)=\frac{1}{12}\left(1-\frac{4M_\pi^2}{s}\right)^{3/2}|F_\pi^{I=1}(s)|^2, \qquad (22)$$

one can include the additional data in order to improve the precision of the moments (21), in particular for the IMSR in which the low-energy region is emphasized. Figure 3 shows the vector spectral function from τ data (three bins) together with the NA7 measurements for energy-squared $s\leqslant0.2$ GeV^2. In addition, we give the result when fitting both data sets using the parametrization

$$F_\pi(s)=1+\frac{1}{6}\langle r^2\rangle_\pi s+As^2+Bs^3, \qquad (23)$$

for the pion form factor. Here, the pion charge radius-squared, $\langle r^2\rangle_\pi=(0.439\pm0.008)$ fm^2, is taken from an analy-

TABLE II. Sum of experimental and theoretical correlations between the moments $R^{(k,l)}_{\tau,V-A}$.

(k,l)	$(1,-1)$	$(0,0)$	$(1,0)$	$(1,1)$	$(1,2)$	$(1,3)$
$(1,-1)$	1	0.46	0.61	0.40	0.26	0.13
$(0,0)$	-	1	0.89	0.97	0.84	0.80
$(1,0)$	-	-	1	0.88	0.74	0.45
$(1,1)$	-	-	-	1	0.89	0.78
$(1,2)$	-	-	-	-	1	0.76

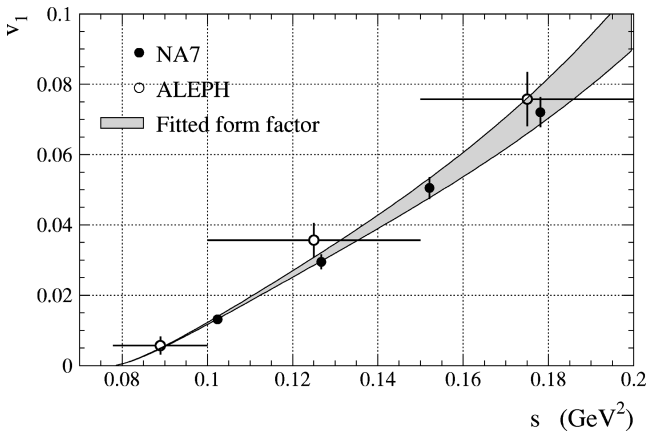

FIG. 3. Low energy vector spectral functions from τ decays and, via CVC, from $e^+e^-\to\pi^+\pi^-$ data measured by NA7 [36].

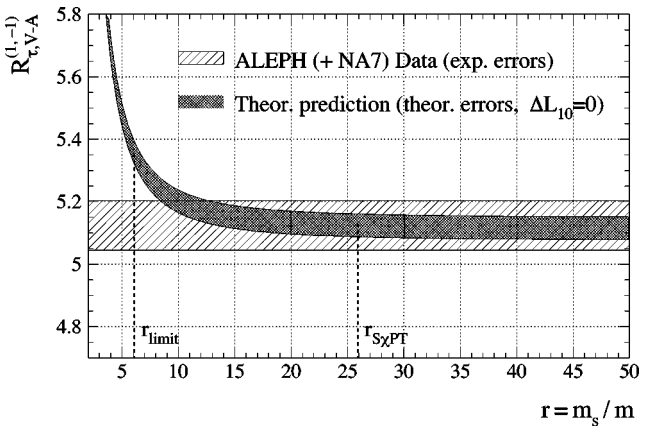

FIG. 4. Theoretical prediction of the IMSR moment $R^{(1,-1)}_{\tau,V-A}$, using $L_{10}^{\rm eff}=-6.36\times10^{-3}$ as fixed input value, versus the mass ratio r. The theoretical uncertainty stems mainly from the error on $\alpha_s(M_\tau^2)$. The dashed band shows the $(V-A)$ data from hadronic τ decays (including low energy e^+e^- vector cross sections) within experimental errors.

sis of space-like data [37]. We stress that the form (23), which does not correspond to the actual analytic behavior of the form factor at low energy, is merely used as a parametrization of experimental data. We obtain the fit results $A=-(7.5\pm1.1)$ GeV^{-4} and $B=(62.5\pm6.4)$ GeV^{-4} with $\chi^2=0.6$ for 5 degrees of freedom. The correlation between A and B is absorbed in the diagonal errors given, so that both quantities can be handled as being uncorrelated. Replacing for the above energy interval $4M_\pi^2\leqslant s\leqslant0.2$ GeV^2 the pure τ data by a combination of τ and e^+e^- data represented by the analytical expressions (22) and (23), we obtain the results given in the third and fourth line of Table I. A small improvement in precision of 11% is observed for the IMSR.

The spectral information is used to fit simultaneously the low-energy quantity $L_{10}^{\rm eff}$ and the nonperturbative phenomenological operators. For dimension $D=6$ we will neglect the contribution of $\mathcal{O}_6^2$, which is suppressed by α_s^2 and, furthermore, is suppressed relatively to $\mathcal{O}_6^1$ in the large N_c limit. Therefore we will simply keep $\mathcal{O}_6=\mathcal{O}_6^1(M_\tau^2)$ and the $\mathcal{O}_8$ operator of dimension $D=8$.

VI. RESULTS OF THE FIT

The fit minimizes the χ^2 of the differences between measured and fitted quantities contracted with the inverse of the sum of the experimental and theoretical covariance matrices taken from Table II. The results of the fit are, for $L_{10}^{\rm eff}$,

$$L_{10}^{\rm eff}=-(6.36\pm0.09_{\rm exp}\pm0.14_{\rm theo}\pm0.07_{\rm fit}\pm0.06_{\rm OPE})\times10^{-3}, \tag{24}$$

and, for the nonperturbative operators,

$$\langle\mathcal{O}_6\rangle=(5.0\pm0.5_{\rm exp}\pm0.4_{\rm theo}\pm0.2_{\rm fit}\pm1.1_{\rm OPE})\times10^{-4}\ {\rm GeV}^6, \tag{25}$$

$$\langle\mathcal{O}_8\rangle=(8.7\pm1.0_{\rm exp}\pm0.1_{\rm theo}\pm0.6_{\rm fit}\pm2.1_{\rm OPE})\times10^{-3}\ {\rm GeV}^8, \tag{26}$$

with a χ^2 of 2.5 for 3 degree of freedom. The errors are separated in experimental (first number) and theoretical (second number) parts, and a fit uncertainty (third number) is added. The latter is due to a well known bias when fitting quantities for which correlations are due to normalization uncertainties [38] (here the τ branching ratios) leading systematically to lower values in terms of the normalization of the fitted parametrization. The errors quoted account for the differences between fully correlated and uncorrelated results. Notice that the theoretical error for $L_{10}^{\rm eff}$ comes mostly from the uncertainty in the quark mass ratio r (sixth line of Table I), which we generously allowed to range in the whole interval $8<r<\infty$. If one believes, for instance, the standard picture of chiral symmetry breaking ($r\sim25$), this error would be negligible, as is clear from Fig. 4. In this case the theoretical error in Eq. (24) should be reduced to $\pm0.03_{\rm theo}$. The authors of Ref. [7] observed a variation of the results on the nonperturbative operators depending on the weighting of the τ spectral functions used in the actual fit. These variations stem from deviations between data and the OPE approach for the running $R_{\tau,V/A}(s_0\leqslant M_\tau^2)$ in the vector and axial-vector channels (visualized in Fig. 17 of Ref. [7]) and from the correlation between the fitted dimension $D=6$ and $D=8$ operators. They have been found to be larger than the theoretical and experimental uncertainties. We repeat this study here in order to estimate the corresponding systematic uncertainties for the fitted quantities. The last numbers in Eqs. (24)–(26), denoted as ''OPE'' errors, give the deviations found. They are small for $L_{10}^{\rm eff}$ and dominant for the nonperturbative operators.

Table III gives the correlations between the fitted parameters which are found to be small. Nevertheless, the interpretation of the parameter errors given in Eqs. (24)–(26) as individual errors must be done with care in the presence of non-vanishing correlations. The results can reliably be used when applying the whole expansion (8) which yields Eqs. (16) and (17).

Expressing $L_{10}^{\rm eff}$ of Eq. (24) by means of Eq. (19) at the χPT renormalization scale $\mu_{\chi\rm PT}=770$ MeV, we obtain

TABLE III. Correlations between the fitted parameters (24)–(26).

	L_{10}	$\langle\mathcal{O}_6\rangle$	$\langle\mathcal{O}_8\rangle$
L_{10}	1	−0.26	0.05
$\langle\mathcal{O}_6\rangle$	-	1	0.14

$$L_{10}^r(M_\rho) = -(5.13 \pm 0.19) \times 10^{-3}. \quad (27)$$

The same central value, with smaller error,

$$L_{10}^r(M_\rho) = -(5.13 \pm 0.13) \times 10^{-3}, \quad (28)$$

would result if one excludes the region $r < 15$ (see Fig. 4), for the quark mass ratio. Note that the quoted errors in Eqs. (27), (28) do not take into account uncertainties from higher order chiral corrections in Eq. (19). In deriving the above value the term $2\hat{m}^2(2B_3 - \hat{H}_{2,2})$ in Eq. (19) has been neglected. Naive dimensional analysis estimates [39] give for the low-energy constants B_3 and $H_{2,2}$ an order of magnitude of 10^{-2}, leading to a contribution which is negligible compared to the theoretical error in Eq. (24). Previous estimates of the same constant were based on resonance saturation assumptions [40] and on an evaluation of the DMO sum rule (1) [41], leading, respectively, to $L_{10}^r(M_\rho) = -6.0 \times 10^{-3}$ and $L_{10}^r(M_\rho) = -4.3 \times 10^{-3}$. Our result (27) represents an improvement of these estimates. Alternative determinations rely on the analysis of $\pi \to e\nu\gamma$ decays and $\langle r^2 \rangle_\pi$. The one-loop value of L_{10} extracted in this way is reported in Ref. [42],

$$L_{10}^r(M_\rho) = (-5.5 \pm 0.7) \times 10^{-3}. \quad (29)$$

Two-loop calculations of both $\pi \to e\nu\gamma$ [43] and, more recently, pion form factors [44], have been completed. These analyses were carried out in the SU(2)×SU(2) formalism, thus determining the SU(2) constant l_5, instead of L_{10}, which is the corresponding one for SU(3). Since the correspondence between the two sets of constants is only known at one-loop level [22], we can rewrite our result for L_{10} as

$$\overline{l}_5 = 13.08 \pm 0.36, \quad (30)$$

and compare it to the two loop value $\overline{l}_5 = 13.0 \pm 0.9$ found in Ref. [44]. This means that the constant l_5 extracted from $\pi \to e\nu\gamma$ approaches, at two-loop level, our one-loop value of Eq. (30), extracted from τ decays. Using the result of Refs. [23, 24] one could find the relation between L_{10}^r and $L_{10}^{\rm eff}$ defined in Eq. (18) at two-loop level. However, as already pointed out in Ref. [9], one is faced with the appearance of $O(p^6)$ constants, whose contribution to $L_{10}^{\rm eff}$ can hardly be disentangled from L_{10}^r.

The total, purely nonperturbative contribution to $R_{\tau,V-A}$ found in the fit, taking into account the correlations between the operators, amounts to

$$R_{\tau,V-A} = 0.061 \pm 0.014, \quad (31)$$

compared to the measurement $R_{\tau,V-A} = 0.055 \pm 0.031$. The reduced error of the theoretical fit to data compared to the measurement stems from the additional information used in the fit which is obtained from the shape of the spectral functions and the OPE constraint. The result (31) is in good agreement with the value of $R_{\tau,V} - R_{\tau,A} = 0.068$ found in Ref. [7]. This is a non-trivial result keeping in mind the logarithmic s dependence of the dimension $D=6$ Wilson coefficients used in this analysis compared to the vacuum saturation hypothesis adopted in Ref. [7]. In addition, in Ref. [7], vector and axial-vector were not combined in a simultaneous fit. The smaller systematic error on the nonperturbative parts which is found in this analysis, in particular the reduced uncertainty from the explicit dependence of the moments employed, is due to the reduced correlation between the fitted $D=6$ and $D=8$ operators (see Table III). The dimension $D=6$ contribution to $R_{\tau,V-A}$ corresponding to our fit result Eq. (25) amounts to $R_{\tau,V-A}^{(D=6)} = 0.071 \pm 0.018$, which is significantly larger than what one obtains from the vacuum saturation hypothesis [14], $R_{\tau,V-A}^{(D=6)} \simeq 0.97 \times 256\pi^3 \alpha_s \langle\overline{q}q\rangle^2 / M_\tau^6 \approx 0.012$.

In addition to the test of the OPE by varying the (k,l) moments used to fit $L_{10}^{\rm eff}$ and the nonperturbative operators, we perform fits for variable ''τ masses'' $s_0 \leqslant M_\tau^2$ [7] which provides a direct test of the parameter stability at M_τ^2. In order to perform such a study one has to replace all τ masses in Eqs. (7), (17), and (21) by s_0, while the latter must be corrected by the kinematical factor $(1 - s/s_0)^2(1 + 2s/s_0)/s_0$. The scale invariance of the dimension $D=6$ operator for variable s_0 is approximately conserved when keeping the scale parameter $\mu = M_\tau$ in Eqs. (9) and (17) unchanged. The dimension $D=8$ operator is assumed to be scale invariant. Figure 4 shows the fitted observables as a function of s_0. The horizontal bands give the results at M_τ^2

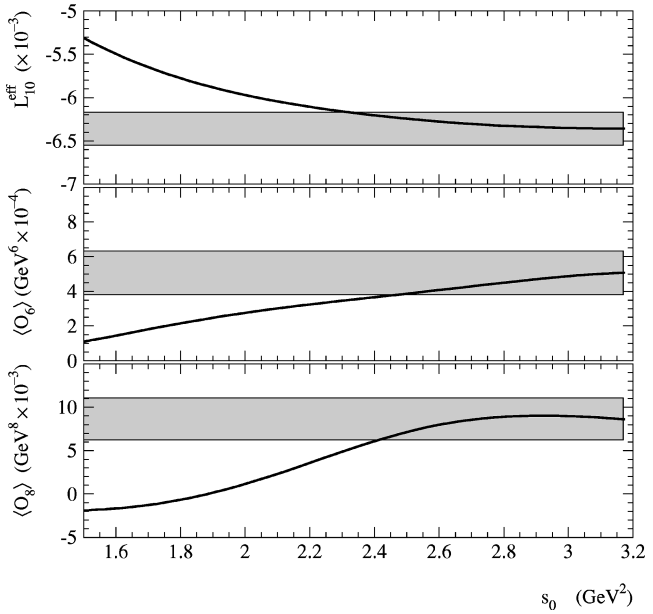

FIG. 5. Fit results for $L_{10}^{\rm eff}$ and the nonperturbative operators as a function of the ''τ mass'' s_0. The bands depict the values (24)–(26) within errors, obtained at M_τ^2.

within one standard deviation. All curves show a convergent behavior for $s_0 \to M_\tau^2$. Any deviation from the fitted values for $s_0 > M_\tau^2$ should be covered by the ''OPE'' errors assigned to the results (24)–(26).

Since we use GχPT formulas in this analysis we have investigated the sensitivity of the $(V-A)$ τ data to a possible constraint on the mass ratio r itself. Clearly a combined fit of $L_{10}^{\rm eff}$, r and the nonperturbative operators must fail due to the strong correlations of the input variables which reduce the effective degrees of freedom of the fit. Thus, as a test, we may use as input for $L_{10}^{\rm eff}$ and the nonperturbative operators the values (24)–(26) and assume them to be perfectly known, e.g., from a precise second measurement. Figure 5 shows the theoretical prediction of the (most sensitive) IMSR moment $R_{\tau,V-A}^{(1,-1)}$ as a function of r within the errors from the other theoretical sources given in Table I, dominated by the error on α_s. Additionally shown as a horizontal band are the ALEPH data within experimental errors. We conclude that the current experimental precision of the non-strange data does not allow to constrain the light quark masses, i.e., the mass ratio r. In the limit of zero u,d quark masses $(r \to \infty)$ we obtain $R_{\tau,V-A}^{(1,-1)} = 5.11$ which is still within the data band of one experimental and theoretical standard deviation. The sensitivity on r when employing the $l \geqslant 0$ moments is even worse than with the IMSR.

VII. CONCLUSIONS

This paper deals with a combination of finite energy sum-rule techniques and chiral perturbation theory (χPT) low-energy expansion in order to exploit recent ALEPH data on the non-strange τ vector and axial-vector spectral functions with respect to an experimental determination of the χPT quantity L_{10}. The theoretical predictions of the spectral moments, $R_{\tau,V-A}^{(k,l)}$, of the τ hadronic width involve nonperturbative elements of the operator product expansion when calculating the contour integral at $|s| = M_\tau^2$. In the case of inverse spectral moments $(l<0)$, additional χPT parameters appear originating from a second contour integral at the $|s| = 4M_\pi^2$ production threshold which subtracts the singularity of the $(s/M_\tau^2)^{-1}$ inverse moment at $s=0$. A constrained fit of $l<0$ and $l \geqslant 0$ spectral moments adjusts simultaneously the parameter $L_{10}^{\rm eff}$, defined by Eq. (18), and nonperturbative power operators of dimensions $D=6$ and $D=8$. We obtain $L_{10}^{\rm eff} = -(6.36 \pm 0.09 \pm 0.16) \times 10^{-3}$, where the first error is of experimental and the second of theoretical origin. The present determination of $L_{10}^{\rm eff}$ is independent of any chiral expansion; in particular, the value obtained here can be directly used in a two-loop analysis: it suffices to include higher order corrections in Eq. (19). Within the one-loop χPT the above result corresponds to $L_{10}^r(M_\rho) = -(5.13 \pm 0.19) \times 10^{-3}$, in good agreement with the value $L_{10}^r(M_\rho) = -(5.5 \pm 0.7) \times 10^{-3}$ extracted from the one-loop analyses of $\pi \to e\nu\gamma$ data and $\langle r^2 \rangle_\pi$. The recent extension of these analyses to two-loop level (Refs. [43, 44]) even improves this agreement. The compatibility of the two independent determinations of L_{10} provides a non-trivial test of chiral symmetry underlying χPT. The total nonperturbative prediction to $R_{\tau,V-A}$ found in the fit is in agreement with the values of the ALEPH $\alpha_s(M_\tau^2)$ analysis [7]. The stability of the fit results is investigated in performing various fits for ''τ masses'' smaller than M_τ. Satisfactory convergence is observed.

[1] K. G. Wilson, Phys. Rev. **179**, 1499 (1969).
[2] M. A. Shifman, A. L. Vainshtein, and V. I. Zakharov, Nucl. Phys. **B147**, 385 (1979); **B147**, 448 (1979); **B147**, 519 (1979).
[3] S. Weinberg, Physica A **96**, 327 (1979).
[4] J. Gasser and H. Leutwyler, Ann. Phys. (N.Y.) **158**, 142 (1984).
[5] J. F. Donoghue and E. Golowich, Phys. Rev. D **49**, 1513 (1994).
[6] ALEPH Collaboration, R. Barate *et al.*, Z. Phys. C **76**, 15 (1997).
[7] ALEPH Collaboration, R. Barate *et al.*, Eur. Phys. J. C **4**, 409 (1998).
[8] T. Das, V. S. Mathur, and S. Okubo, Phys. Rev. Lett. **19**, 859 (1967).
[9] E. Golowich and J. Kambor, Phys. Lett. B **421**, 319 (1998).
[10] F. Le Diberder and A. Pich, Phys. Lett. B **289**, 165 (1992).
[11] ALEPH Collaboration, D. Buskulic *et al.*, Phys. Lett. B **307**, 209 (1993).
[12] CLEO Collaboration, T. Coan *et al.*, Phys. Lett. B **356**, 580 (1995).
[13] E. Golowich and J. Kambor, Phys. Rev. D **53**, 2651 (1996).
[14] E. Braaten, S. Narison, and A. Pich, Nucl. Phys. **B373**, 581 (1992).
[15] A. Höcker, thesis, Orsay, France, 1997.
[16] K. G. Chetyrkin and A. Kwiatkowski, Z. Phys. C **59**, 525 (1993).
[17] V. I. Zakharov, Nucl. Phys. **B385**, 452 (1992).
[18] S. Peris and E. de Rafael, Nucl. Phys. **B500**, 325 (1997).
[19] S. C. Generalis, J. Phys. G **15**, L225 (1989).
[20] K. G. Chetyrkin, S. G. Gorishny, and V. P. Spiridonov, Phys. Lett. **160B**, 149 (1985).
[21] L. V. Lanin, V. P. Spiridonov, and K. G. Chetyrkin, Yad. Fiz. **44**, 1372 (1986) [Sov. J. Nucl. Phys. **44**, 892 (1986)].
[22] J. Gasser and H. Leutwyler, Nucl. Phys. **B250**, 465 (1985).
[23] E. Golowich and J. Kambor, Nucl. Phys. **B447**, 373 (1995).
[24] E. Golowich and J. Kambor, Phys. Rev. D **58**, 036004 (1998).
[25] M. Knecht and J. Stern, in *The Second DAΦNE Physics Handbook*, edited by L. Maiani, G. Pancheri, and N. Paver (INFN, Frascati, 1995), Vol. I, p. 169.
[26] S. Weinberg, *A Festschrift for I. I. Rabi*, edited by L. Motz (New York Academy of Sciences, New York, 1977).
[27] N. H. Fuchs, H. Sazdjian, and J. Stern, Phys. Lett. B **238**, 380 (1990); **269**, 183 (1991).
[28] M. Knecht (unpublished).
[29] J. Stern, hep-ph/9712438.

[30] S. Chen, talk given at QCD'97, Montpellier, France, 1997.
[31] D. Ward, talk given at the International Europhysics Conference on High-Energy Physics (HEP 97), Jerusalem, Israel, 1997.
[32] M. Davier and A. Höcker, Phys. Lett. B **419**, 419 (1998).
[33] Particle Data Group, R. M. Barnett *et al.*, Phys. Rev. D **54**, 1 (1996).
[34] W. J. Marciano and A. Sirlin, Phys. Rev. Lett. **56**, 22 (1986); **61**, 1815 (1986).
[35] R. Alemany, M. Davier, and A. Höcker, Report LAL 97-02, 1997; Eur. Phys. J. C (to be published).
[36] NA7 Collaboration, S. R. Amendolia *et al.*, Phys. Lett. **138B**, 454 (1984).
[37] NA7 Collaboration, S. R. Amendolia *et al.*, Nucl. Phys. **B277**, 168 (1986).
[38] G. D'Agostini, Nucl. Instrum. Methods Phys. Res. A **346**, 306 (1994).
[39] H. Georgi, Phys. Lett. B **298**, 187 (1993).
[40] G. Ecker, J. Gasser, A. Pich, and E. de Rafael, Nucl. Phys. **B321**, 311 (1989).
[41] J. F. Donoghue and B. R. Holstein, Phys. Rev. D **46**, 4076 (1992).
[42] J. Bijnens, G. Ecker, and J. Gasser, *The Second DAΦNE Physics Handbook* (Ref. [25]), p. 125.
[43] J. Bijnens and P. Talavera, Nucl. Phys. **B489**, 387 (1997).
[44] J. Bijnens, G. Colangelo, and P. Talavera, J. High Energy Phys. **5**, 14 (1998).